The EMBO Journal Vol.17 No.1 pp.159–169, 1998

Overexpression of a kinase-inactive ATR protein causes sensitivity to DNA-damaging agents and defects in cell cycle checkpoints

William A.Cliby[1,2], Christopher J.Roberts[1,3], Karlene A.Cimprich[4,5], Cheri M.Stringer[1], John R.Lamb[1], Stuart L.Schreiber[3] and Stephen H.Friend[1,6]

[1]The Seattle Project, Program in Molecular Pharmacology, Fred Hutchinson Cancer Research Center, Seattle, WA 98104 and [4]Howard Hughes Medical Institute, Department of Chemistry and Chemical Biology, Harvard University, 12 Oxford Street, Cambridge, MA 02138, USA

[2]Present address: Mayo Clinic, Division of Gynecologic Surgery, Department of Obstetrics and Gynecology, 200 1st Street SW, Rochester, MN 55905, USA
[3]Present address: Rosetta Inpharmatics, Inc., 12040 115th Avenue NE, Kirkland, WA 98034, USA
[5]Present address: Department of Molecular Pharmacology, Stanford University School of Medicine, Stanford, CA 94305–5332, USA

[6]Corresponding author

ATR, a phosphatidylinositol kinase-related protein homologous to ataxia telangiectasia mutated (ATM), is important for the survival of human cells following many forms of DNA damage. Expression of a kinase-inactive allele of ATR (ATRkd) in human fibroblasts causes increased sensitivity to ionizing radiation (IR), *cis*-platinum and methyl methanesulfonate, but only slight UV radiation sensitivity. ATRkd overexpression abrogates the G_2/M arrest after exposure to IR, and overexpression of wild-type ATR complements the radioresistant DNA synthesis phenotype of cells lacking ATM, suggesting a potential functional overlap between these proteins. ATRkd overexpression also causes increased sensitivity to hydroxyurea that is associated with microtubule-mediated nuclear abnormalities. These observations are consistent with uncoupling of certain mitotic events from the completion of S-phase. Thus, ATR is an important component of multiple DNA damage response pathways and may be involved in the DNA replication (S/M) checkpoint.

Keywords: ATR protein/cell cycle checkpoint/DNA damage/hydroxyurea/ionizing radiation

Introduction

Eukaryotic cells employ checkpoints to help ensure the orderly progression and completion of critical events such as DNA replication and chromosome segregation (Elledge, 1996; Paulovich *et al.*, 1997). Checkpoints have been identified that lead to cell cycle arrest after DNA damage (Jackson, 1996b; Lydall and Weinert, 1996), inhibition of DNA replication (Stewart and Enoch, 1996) or disruption of the spindle (Rudner and Murray, 1996). Acting at different points in the cycle, these checkpoints delay transitions from G_1 to S, G_2 to M or inhibit DNA replication during S-phase, depending on the nature of the insult. Presumably, these delays allow time for repair processes or halt cell cycle progression until completion of a critical cell cycle event. Defects in checkpoint genes often result in increased sensitivity to damaging agents and increased genomic instability. Genomic instability is commonly observed in cancer (reviewed by Hartwell and Kastan, 1994; Kinzler and Vogelstein, 1996), and it has been suggested that checkpoint defects might explain this instability. The link between checkpoint defects and cancer is best illustrated by the observation that over half of all human tumors harbor mutations in the *p53* gene (Levine, 1997), which mediates arrest in the G_1/S-phase of the cell cycle in response to DNA damage or rNTP depletion (Kastan, 1996; Linke *et al.*, 1996).

An important upstream component of the p53-dependent DNA damage response pathway is ataxia telangiectasia mutated (ATM; Savitsky *et al.*, 1995) a member of the phosphatidylinositol kinase (PIK)-related kinase family (Keith and Schreiber, 1995). The genetic syndrome ataxia telangiectasia (AT) is characterized by progressive neurodegeneration, extreme sensitivity to ionizing radiation (IR) and a cancer-prone phenotype (Meyn, 1995; Hawley and Friend, 1996). Cells from AT individuals show an increased rate of chromosomal recombination and are defective in the IR-inducible G_1/S (Kastan *et al.*, 1992), S-phase (Painter and Young, 1980) and G_2/M checkpoints (Paules *et al.*, 1995). While ATM plays a key role in the response to IR, AT fibroblasts show little or no hypersensitivity to UV radiation, alkylating agents or inhibitors of DNA replication. This suggests that other proteins are needed for the checkpoint response to different forms of DNA damage.

The PIK-related kinase family are large proteins (2000–4000 amino acids) with carboxy-terminal PIK-related domains (Carr, 1997; Hoekstra, 1997). Members of this family include DNA-PK, which is required for V(D)J recombination and double strand break repair (Weaver, 1995, Jackson, 1996a), and the TOR proteins (TOR1, TOR2 of *Saccharomyces cerevisiae* and mammalian FRAP) which are the targets of the FKBP–rapamycin complex and are required for a signal transduction pathway that mediates G_1 progression in response to nutrient deprivation (Brown and Schreiber, 1996; Hall, 1996). Several other PIK-related kinases contain an additional region of homology known as the Rad3 homologous region, including *S.cerevisiae* MEC1 ($MEC1^{Sc}$; Kato and Ogawa, 1994; Weinert *et al.*, 1994) and TEL1 ($TEL1^{Sc}$; Greenwell *et al.*, 1995; Morrow *et al.*, 1995), *Schizosaccharomyces pombe* Rad3 ($Rad3^{Sp}$; Bentley *et al.*, 1996) and *Drosophila melanogaster* mei-41 (Hari *et al.*, 1995). $mec1^{Sc}$ mutants are defective for G_1, S and G_2/M DNA damage checkpoints and display hypersensitivity to IR,

UV and methyl methanesulfonate (MMS) (Kato and Ogawa, 1994; Weinert *et al.*, 1994; Paulovich and Hartwell, 1995; Sanchez *et al.*, 1996; Siede *et al.*, 1996). *rad3*^{Sp} mutants are sensitive to IR and UV and are deficient for the G_2/M DNA damage checkpoint (Jimenez *et al.*, 1992; Seaton *et al.*, 1992; Bentley *et al.*, 1996). *mei-41* mutants are defective for the G_2/M DNA damage checkpoint and are sensitive to IR (Hari *et al.*, 1995). *MEC1*^{Sc} and *Rad3*^{Sp} are also required for the DNA replication (S/M) checkpoint (Elledge, 1996; Stewart and Enoch, 1996), and mutations in these genes result in hydroxyurea (HU) sensitivity and inappropriate entry into mitosis with an incompletely replicated genome. This checkpoint has also been described in *Xenopus* egg cell-free extracts (Dasso and Newport, 1990; Kumagai and Dunphy, 1995; reviewed in Lew and Kornbluth, 1996).

A recent addition to the Rad3 homology subgroup of the PIK-related kinases has been named FRP1 (for FRAP-related protein) (Cimprich *et al.*, 1996) and ATR (for ATM- and Rad3-related) (Bentley *et al.*, 1996). Evidence for functional homology to other family members includes the demonstration that expression of ATR can complement the UV sensitivity of a *mec1*^{Sc} mutant (Bentley *et al.*, 1996). The additional observation that ATR localizes to unsynapsed meiotic chromosomes (Keegan *et al.*, 1996) suggests that, as is true for the homologous yeast proteins and mei-41, ATR may play a role in meiotic recombination. Given ATR's homology to ATM and the other PIK-related kinases with known checkpoint functions, we investigated whether ATR plays a role in the DNA damage and/or replication response pathways.

Every member of the PIK-related kinase family investigated thus far has been shown to have a critical requirement for an intact kinase domain, including TOR1^{Sc} (Zheng *et al.*, 1995), TOR2^{Sc} (Schmidt *et al.*, 1996), FRAP (Brown *et al.*, 1995), Rad3^{Sp} (Bentley *et al.*, 1996) and MEC1^{Sc} (T.B.Shin and S.L.Schreiber, unpublished results). To examine the function of ATR, our experimental approach is to overexpress a presumptive dominant-negative kinase-inactive allele of ATR, ATR kinase-dead (ATRkd), in a human cell line. We suspected that overexpression of ATRkd would be dominant acting for the following reasons: (i) as noted above, whenever studied, the kinase domains of the PIK-related family members have been found to be essential for function; (ii) overexpression of kinase-dead mutant proteins frequently results in a dominant-negative phenotype, presumably due to the titration of interacting factors (e.g. Perlmutter and Alberola-Ila, 1996). Indeed, kinase-dead alleles of TOR1, TOR2 and Rad3 are dominant-negative when overexpressed (Zheng *et al.*, 1995; Bentley *et al.*, 1996; Schmidt *et al.*, 1996). However, our approach, and subsequent interpretations, assume the observations are ascribed to loss of wild-type ATR function; the possibility that overproduction of ATRkd may exert an effect on other proteins must be kept in mind.

We find that human cells overexpressing ATRkd have increased sensitivity to several DNA-damaging agents, are unable to arrest at the G_2/M checkpoint in response to IR and show increased sensitivity and gross nuclear abnormalities after exposure to HU. These phenotypes are similar to *mec1*^{Sc} and *rad3*^{Sp} mutants, underscoring the functional conservation among eukaryotic PIK-related kinase family members in their roles in DNA damage response pathways. The additional observation that overexpression of wild-type ATR complements the radioresistant DNA synthesis (RDS) phenotype of AT cells suggests that there is functional overlap between ATR and ATM.

Results

Doxycycline-inducible expression of wild-type and kinase-dead ATR in GM847 fibroblasts

Following the rationale noted above, we engineered a mutant form of the ATR cDNA that contains a putative kinase-inactivating mutation. We utilized the inducible tetracycline (tet)- regulatory system (Gossen and Bujard, 1992; Gossen *et al.*, 1995) to control expression of either wild-type or kinase-dead ATR in clones derived from an SV40-transformed fibroblast cell line, GM847. The tet-regulatory system allows selection and maintenance of clones under conditions where the gene of interest is not expressed until necessary for experimental procedures. The wild-type and kinase-dead cDNAs (referred to as ATRwt and ATRkd, respectively) were tagged with an amino-terminal FLAG epitope, and placed under the control of the tet-promoter (see Materials and methods). The ATR cDNAs were co-transfected with pUHD172.1neo (encoding the rtTA transcriptional activator; Gossen *et al.*, 1995) into GM847 fibroblasts, and clones displaying highly regulated expression of FLAG-tagged ATRwt and ATRkd were isolated (Figure 1A). We have referred to stable transfected cell lines in the following manner: cell line/transfected tet-regulatory ATR construct (doxycycline status). For example, GM847/ATRwt(+) represents the GM847 cell line transfected with the ATRwt construct in the presence of doxycycline. Corresponding Western blots using anti-ATR antibody, which recognizes both the endogenous and FLAG-tagged ATR, were analyzed by densitometry and revealed a 3.3-fold increase in protein expression (Figure 1A), with induction maximized at 16 h after the addition of doxycycline (data not shown). It should be noted that even in the uninduced condition, expression of FLAG-tagged ATR was apparent. No differences in doubling times, viability or cellular morphology were observed in cells expressing increased levels of ATRwt or ATRkd, either with or without doxycycline (data not shown).

To determine whether the ATRkd mutation disrupted ATR kinase activity, *in vitro* protein kinase assays were performed on anti-FLAG-immunoprecipitated ATRwt and ATRkd. Upon incubation with [γ-^{32}P]ATP, a phosphorylated species that co-migrated with ATR was present in the immunoprecipitate from GM847/ATRwt(+) cells, but not from those of the GM847 or the GM847/ATRkd(+) cells (Figure 1C). Thus, as suggested previously (Keegan *et al.*, 1996), ATRwt was able to undergo autophosphorylation *in vitro*. Previous experiments, however, did not show this activity to be intrinsic. It is shown here that mutation of Asp2475 to Ala abolished this phosphorylation, indicating that the activity is dependent upon the kinase domain of ATR.

ATRkd overexpression sensitizes cells to several DNA-damaging agents

To determine whether ATR kinase activity is important for survival after DNA damage, we performed clonogenic

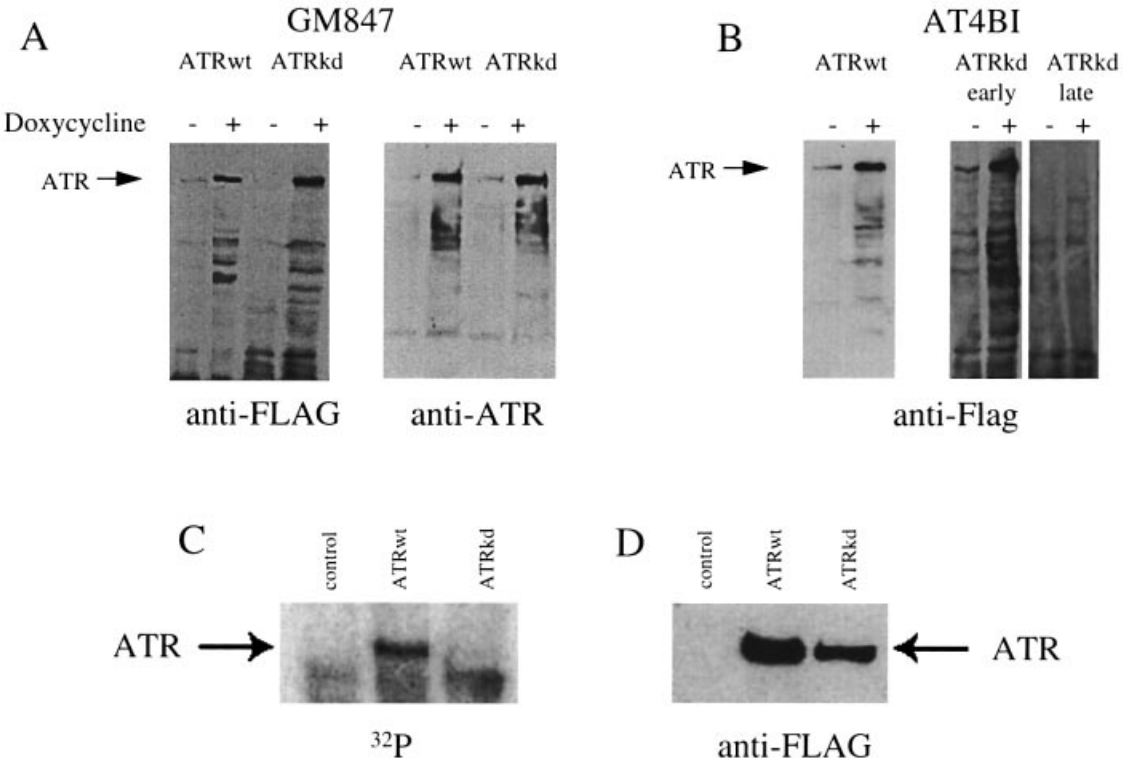

Fig. 1. Inducible expression of ATRwt and ATRkd in GM847 and AT4BI fibroblasts. Immunodetection of ATRwt and ATRkd, in the presence (+) or absence (–) of doxycycline in (**A**) a transfected GM847 cell line using anti-FLAG antibody and anti-ATR antibody and (**B**) a transfected AT4BI cell line using anti-FLAG antibody. Immunodetection of AT4BI/ATRkd clones when isolated (early), and after several passages (late) is shown. *In vitro* autophosphorylation assay of ATRwt and ATRkd in GM847 fibroblasts. FLAG-tagged ATR was immunoprecipitated using anti-FLAG antibody and (**C**) incubated with [γ-^{32}P]ATP or (**D**) analyzed by immunodetection.

survival assays on GM847 fibroblasts, GM847/ATRwt(+) and GM847/ATRkd(+/–) cells after exposure to IR, MMS *cis*-platinum and UV (Figure 2A–D). Expression of ATRkd renders cells very sensitive to *cis*-platinum and MMS, more sensitive to IR than the parental control, and slightly more sensitive to UV. There was a plateau noted for the GM847/ATRkd(+) cells tested against *cis*-platinum, suggesting that a percentage of cells were resistant to this agent. The increased sensitivity to IR was less than that seen in an ATM-deficient fibroblast line (AT3BI; Figure 2A). Thus, these results demonstrate that overexpression of ATRkd interferes with the cell's response to some but not all types of DNA damage, suggesting that ATR plays an important role in DNA damage response pathways.

ATR and the radiation-induced G_2/M arrest

To analyze the role of ATR in the G_2 arrest after exposure to ionizing radiation, we utilized the following assay. Twenty four hours after plating, asynchronously growing cells were exposed to 8 Gy of IR and the microtubule poison nocodazole was added. Sixteen hours later, cells stained with propidium iodide were examined by fluorescence-activated cell sorting (FACS) to determine cell cycle distribution. To distinguish the relative contribution of G_2 and M-phase cells to the G_2/M peak seen by FACS, mitotic spreads were counted from parallel samples. The number of G_2 cells was determined by subtraction of the M-phase cells from the G_2/M total. This allows quantitation of the percentage of cells in all phases of the cell cycle. In addition, cells that pass through G_2 are blocked at M-phase by nocodazole and prevented from re-entering the subsequent cell cycle. Thus, using this assay, cells with a strong G_2 checkpoint response are represented by a large number of cells in G_2 at 16 h, with few cells progressing to the nocodazole block. In contrast, cells deficient in the G_2 checkpoint have relatively few G_2 arrested cells, with the majority blocked in M-phase with nocodazole.

Figure 3 illustrates the cell cycle response following radiation for the parental (GM847) and GM847/ATRkd (± doxycycline) cell lines. Figure 3A–C shows that the untreated asynchronous cell cycle distributions of the different cell lines examined are similar. Figure 3D–F shows that when treated with nocodazole alone, cells were arrested in mitosis. After exposure to IR alone, all cell lines showed an increase in the percentage of G_2 cells (Figure 3G–I); however, this effect was less dramatic in the GM847/ATRkd(+) cells which have a correspondingly higher percentage of G_1 cells (Figure 3I). By employing the nocodazole block to eliminate cells from passing into the subsequent cell cycle, the truly G_2-arrested population can be delineated more clearly (Figure 3J–L). In GM847 cells with a strong G_2 arrest after IR, few cells reach the nocodazole block (Figure 3J). In contrast, GM847/ATRkd(+) cells fail to arrest in G_2, and the majority of cells proceed into mitosis (Figure 3L). Thus, expression of ATRkd disrupts the G_2/M checkpoint seen after ionizing radiation. The dose of IR used for these experiments was chosen to maximize the G_2 arrest seen. This dose corresponded to a survival of ~1–10% in clonogenic assays (Figure 2A), and an argument could be made that the decrease in the population of ATRkd(+) G_2 arrested

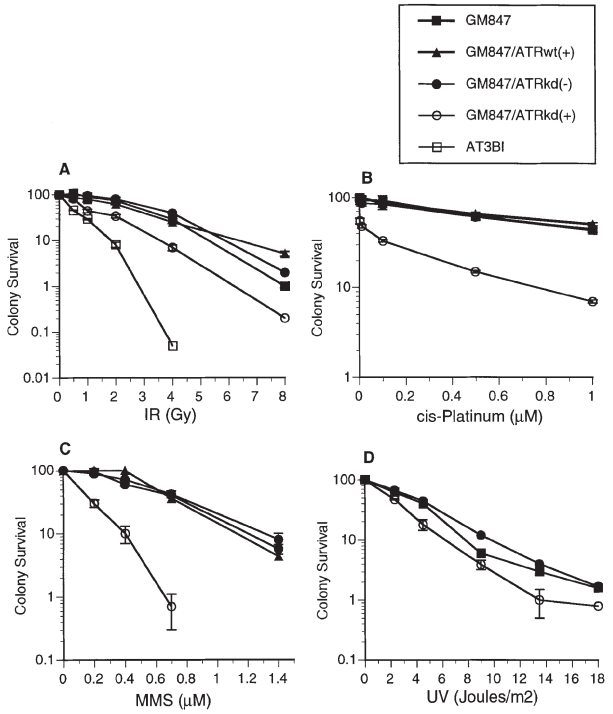

Fig. 2. ATRkd expression renders cells sensitive to several DNA-damaging agents. Clonogenic survival of GM847, GM847/ATRwt, GM847/ATRkd and AT3BI fibroblasts, in the presence (+) or absence (–) of doxycycline, was determined after exposure to increasing doses of the following agents as detailed in Materials and methods: (**A**) IR; (**B**) *cis*-platinum; (**C**) MMS; and (**D**) UV radiation. Plating efficiency was determined for all cell lines and ranged from 12 to16%. All measurements were performed in triplicate, and consistent results were obtained among experiments. In GM847 and GM847/ATRwt cell lines, the clonogenic survival was not affected by the presence or absence of doxycycline; results are shown for cells exposed to doxycycline.

cells seen after IR might be explained by selective killing of this fraction. If this were true, we would have expected to see a sub-2N peak of cells corresponding to apoptotic cells, and we should not have observed the large increase in M-phase cells treated with nocodozole and IR. We therefore feel confident that our findings represent loss of the G_2 arrest.

ATR and radioresistant DNA synthesis (RDS)

Given the structural similarity of ATR and ATM, we wished to investigate whether increased expression of ATR could complement the lack of ATM in AT fibroblasts. We transfected AT fibroblasts (AT4BI) with the tet-regulatory ATRwt- and ATRkd-expressing constructs. Clones were isolated that could express either ATRwt or ATRkd (Figure 1B). Interestingly, the AT4BI/ATRkd(–) clones grew very slowly, producing many dead cells (data not shown). It is important to note the relatively high levels of ATRkd expression even without induction (Figure 1B ATRkd, early, –doxycycline). This period of poor growth of AT4BI/ATRkd clones was followed by the emergence of a population of cells with normal growth characteristics, but which no longer expressed ATRkd (Figure 1B ATRkd, late). Thus, it appears that prolonged ATRkd expression was not tolerated in AT4BI cells, suggesting that expression of ATRkd may be lethal to cells with an ATM defect. Alternatively, given the inherent genomic instability attributed to AT cells, it may be that some secondary defect, unrelated to the primary ATM mutation, is responsible for this apparent non-viable interaction with ATRkd. We were also unable to establish stable clones capable of ATR expression in a breast (MCF-7) or lung (A549) adenocarcinoma cell line (data not shown).

To determine whether ATR is required for IR-induced inhibition of DNA synthesis, we measured [^{3}H]thymidine incorporation into DNA after treatment with 0.5–40 Gy IR. Whereas the AT4BI fibroblasts displayed the classic RDS phenotype, all other lines tested showed inhibition of DNA synthesis similar to the control GM847 cells regardless of ATRkd expression (Figure 4A). We observed that induction of ATRkd overexpression in GM847 fibroblasts resulted in less inhibition of DNA synthesis after IR than that observed in the uninduced ATRkd cells, though not different from the parental GM847 cell line. The relevance of this observation to the role of ATR in the S-phase checkpoint is unclear. Doxycycline had no independent effect on the rates of DNA synthesis after IR in either of the untransfected cell lines (GM847 or AT4BI, data not shown).

To assess whether overexpression of ATRwt is able to restore radiation-induced inhibition of DNA synthesis to AT cells, we performed this assay on AT4BI fibroblasts transfected with the tet-inducible ATRwt construct [Figure 1B; designated AT4BI/ATR(–/+)]. Figure 4B shows that induction of ATRwt overexpression in AT4BI fibroblasts restores the ability of these cells to inhibit DNA synthesis after exposure to IR. We have not evaluated the effect of overexpression of wild-type ATR on AT cells' survival after IR exposure.

ATR and the DNA replication checkpoint

Yeast mutants (e.g. *mec1^{Sc}* and *rad3^{Sp}*) defective for the DNA replication checkpoint are highly sensitive to HU and appear to perform some mitotic functions without completing S-phase (Elledge, 1996). To examine the role of ATR in this checkpoint, we treated GM847 and GM847/ATRkd cells with 1 mM HU, a concentration that results in a >90% decrease in DNA synthesis (data not shown). Figure 5 illustrates clonogenic survival after increasing lengths of exposure to 1 mM HU. The induction of ATRkd expression rendered cells significantly more sensitive to HU when compared with the uninduced GM847/ATRkd(–) and untransfected GM847 cell lines.

Fungal mutants defective for the DNA replication checkpoint display an uncoupling of mitotic events from the completion of DNA replication. In the presence of HU, both *mec1^{Sc}* and *rad3^{Sp}* mutants show an aberrant elongation of the spindle despite having an unreplicated genome (Enoch *et al.*, 1992; Weinert *et al.*, 1994), and *rad3^{Sp}* mutants additionally show a 'cut' phenotype caused by septum formation in the absence of nuclear division. To assess whether the increased HU sensitivity associated with ATRkd expression was due to disruption of the DNA replication checkpoint *per se*, we examined nuclear and spindle morphology, centrosome number and nuclear envelope breakdown after HU exposure. For these experiments, we used GM847 and GM847/ATRkd cell lines (± doxycycline). Cells were treated for increasing amounts of time with 1 mM HU, fixed and analyzed by indirect immunofluorescence using antibodies directed against

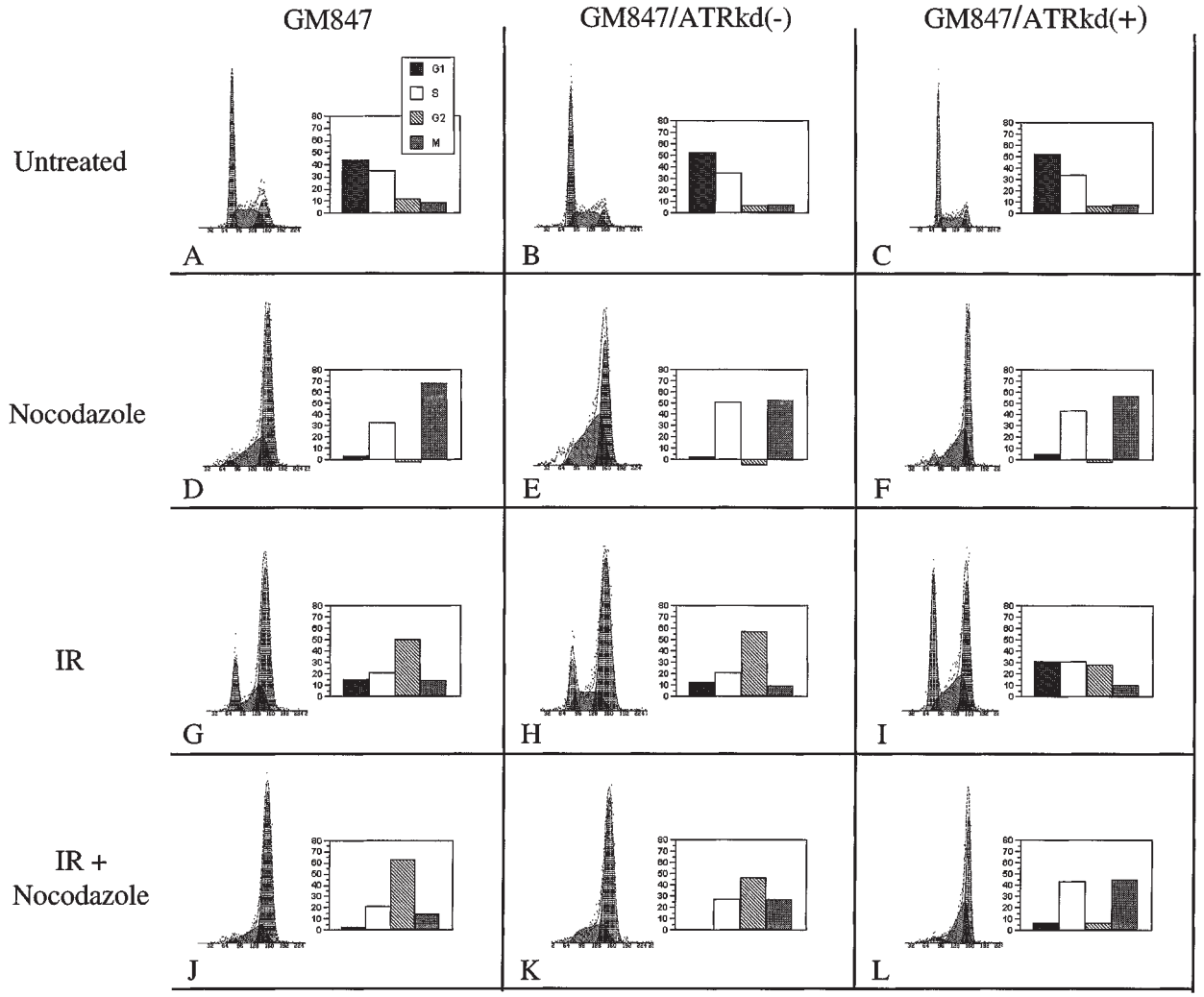

Fig. 3. ATR is required for the IR-induced G_2/M checkpoint. Cell cycle profiles were determined by FACS analysis and mitotic spreads after exposure to IR ± nocodazole for the following cell lines: GM847, GM847/ATRkd(–) and GM847/ATRkd(+). Results were consistent between four independent experiments. Cell cycle distributions are presented for untreated (**A–C**), 16 h after treatment with 0.1 μg/ml nocodazole (**D–F**), 16 h after 8 Gy IR (**G–I**) and 16 h after IR and nocodazole (**J–L**).

α-tubulin, γ-tubulin and lamin B, and the nuclei were counterstained with Hoechst 33258. Figure 6A shows representative GM847 cells after 24 h of HU treatment. The cells displayed interphase-like nuclear and microtubule morphologies, and cells with mitotic spindles disappeared from the population with increasing length of exposure to HU. However, a subpopulation of cells (8.6%; Table I) displayed abnormal nuclear morphologies, independent of HU exposure. The abnormal nuclei were irregular in shape, having multiple lobes and invaginations (Figure 6B and C). The GM847/ATRkd(+) cells displayed a significantly higher incidence of abnormal nuclear morphologies (13.6%) and, in contrast to the GM847 cells, this appearance increased to 30.2% after HU exposure. Similar results were obtained after 24 h of treatment with 20 μM aphidicolin, an inhibitor of DNA polymerases (data not shown).

In cells with abnormal nuclei, we observed that microtubules appeared to be located within the invaginations (Figure 6B and C), suggesting a role for microtubules in their formation. We did not see evidence for a well-defined mitotic spindle. To assess whether formation of the abnormal nuclear shapes was mediated by microtubules, GM847/ATRkd(+) cells were treated with either nocodazole (0.1 μg/ml), HU (1 mM) or both for 24 h (Table IB). In the HU-only-treated cells, the expected ATRkd-dependent abnormal nuclear morphology was present in 27.2% of cells. In contrast, in the cells treated simultaneously with nocodazole and HU, the percentage of abnormal nuclei decreased to 2.7% (Table IB and Figure 6J and K). These data demonstrate that formation of the abnormal nuclear morphology is dependent upon microtubule activity. After treatment with nocodazole, 45.7% of cells showed condensed chromosomes consistent with a mitotic block (Table IA). Treatment of cells with HU in combination with nocodazole reduced the percentage of cells with condensed chromosomes to 2.7%. Therefore, in GM847/ATRkd(+) cells, chromosome condensation does not occur in the absence of genome replication.

To address whether centrosome duplication was uncoupled from the completion of DNA replication, centrosome number and location were determined using anti-γ-tubulin antibody after 6, 12 and 24 h of HU or aphidicolin exposure (Figure 6D–F). No difference was seen regardless of ATRkd expression.

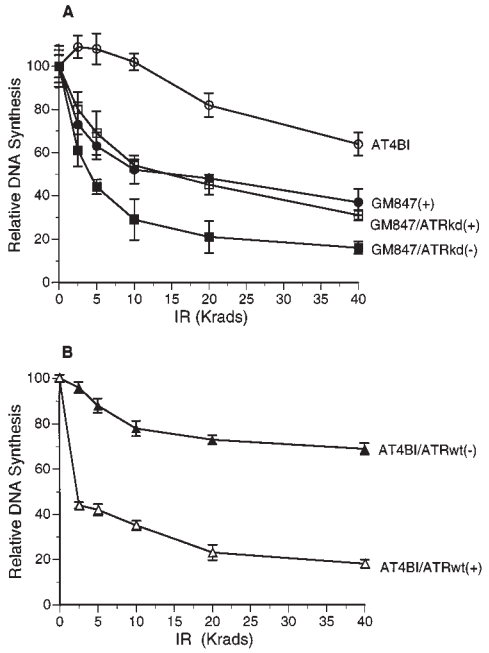

Fig. 4. Radioresistant DNA synthesis assay. Rate of DNA synthesis after exposure to increasing doses of IR. Cells were grown in [^{14}C]thymidine-labeled medium, exposed to graded doses of IR and labeled with [^{3}H]thymidine for 4 h before harvesting for analysis. The relative amounts of DNA synthesis were determined by normalizing the ratio of [^{3}H]thymidine to [^{14}C]thymidine incorporation to the appropriate untreated control. All samples were analyzed in triplicate, and consistent results were obtained among four independent experiments. (**A**) GM847(+), GM847/ATRkd(+/–) and AT4BI(–) cells lines were evaluated. (**B**) GM847(+), and AT4BI/ATRwt(+/–) cell lines were evaluated.

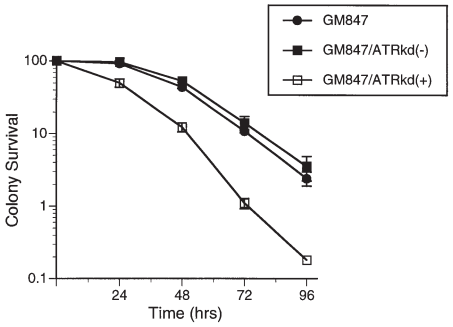

Fig. 5. ATRkd expression confers sensitivity to HU. Clonogenic survival of GM847 and GM847/ATRkd fibroblasts, in the presence (+) or absence (–) of doxycycline, was determined following increasing lengths of exposure to HU. All measurements were performed in triplicate, and consistent results were obtained between experiments.

We also investigated whether the abnormal nuclear morphologies were associated with disruption of the nuclear lamina. The lamin proteins form a subnuclear structure in the perimeter of interphase nuclei (Figure 6G). Upon entry into mitosis, the lamin proteins disassociate, resulting in nuclear envelope breakdown. In cells with abnormal nuclei, lamin B was often absent from the lobed regions (Figure 6H and I). These results show that expression of ATRkd results in increased HU sensitivity, and is associated with microtubule-mediated formation of abnormal nuclei.

Discussion

Using inducible high-level expression of an ATR kinase mutant, we have investigated the role of ATR in DNA damage response pathways. We find that overexpression of ATRkd in GM847 fibroblasts results in increased sensitivity to IR, *cis*-platinum and MMS, but only a slight increase in UV sensitivity (Figure 2), and abrogates the IR-induced G_2 arrest (Figure 3). Overexpression of ATRwt complements the S-phase defect of an AT fibroblast cell line (Figure 4), suggesting overlapping ATR and ATM functions. Additionally, ATRkd-expressing cells are HU sensitive (Figure 5) and develop abnormal microtubule-dependent nuclear morphologies which might represent an uncoupling of certain mitotic events from the completion of DNA replication (Figure 6; Table I). Therefore, ATR, similar to Rad3^{Sp} and MEC1^{Sc}, is an important component of multiple cell cycle checkpoints.

High level expression of kinase-dead mutant forms of the PIK-related kinases Rad3^{Sp}, TOR1^{Sc} and TOR2^{Sc} result in dominant-negative phenotypes (Zheng *et al.*, 1995; Bentley *et al.*, 1996; Schmidt *et al.*, 1996). We cannot say definitively that expression of the dominant acting ATRkd produces a dominant-negative phenotype, since the phenotype of a null mutation at ATR is unknown. However, given the similarities of the phenotypes induced by ATRkd expression and those seen in *mec1^{Sc}* and *rad3^{Sp}* mutants, overexpression of ATRkd is most likely dominant-negative. One important caveat to this approach is that overexpressed ATRkd may perturb the functioning of other proteins and that our observations reflect disruption of those proteins and not loss of wild-type ATR function.

ATR, ATM and the response to ionizing radiation

ATR and ATM are both required for an appropriate cellular response to IR. AT cells are deficient for the IR-induced checkpoints at the G_1, S and G_2 phases of the cell cycle (Painter and Young, 1980; Kastan *et al.*, 1992; Paules *et al.*, 1995). In contrast, ATR is required for G_2/M arrest after IR, and plays little or no role in the IR-induced S-phase checkpoint. We were unable to address the role of ATR in the G_1/S DNA damage checkpoint as the SV40-transformed fibroblast cell line used demonstrates a relatively weak radiation-induced G_1/S arrest (data not shown). The fact that ATM is required for multiple IR-induced checkpoints may account for the greater sensitivity of AT fibroblasts compared with ATRkd-expressing fibroblasts. Remarkably, overexpression of ATRwt complements the RDS phenotype of an AT cell line (Figure 4B). This suggests that there may be functional overlap between ATM and ATR, though we did not investigate the ability of ATRwt to complement the radiation sensitivity of AT cells. Similarly, in *S.cerevisiae*, the related proteins MEC1 and TEL1 may have partially overlapping functions. Although *tel1* cells are not sensitive to IR, UV or HU, double mutant *mec1 tel1* cells are more sensitive than *mec1* cells (Morrow *et al.*, 1995; Sanchez *et al.*, 1996). Additionally, one or two extra copies of *TEL1* in a *mec1* mutant are sufficient partially to suppress these mutant phenotypes. Finally, ATRkd expression was not tolerated in AT cells (Figure 1B), suggesting a requirement for at least one of the two proteins for the viability of human cells.

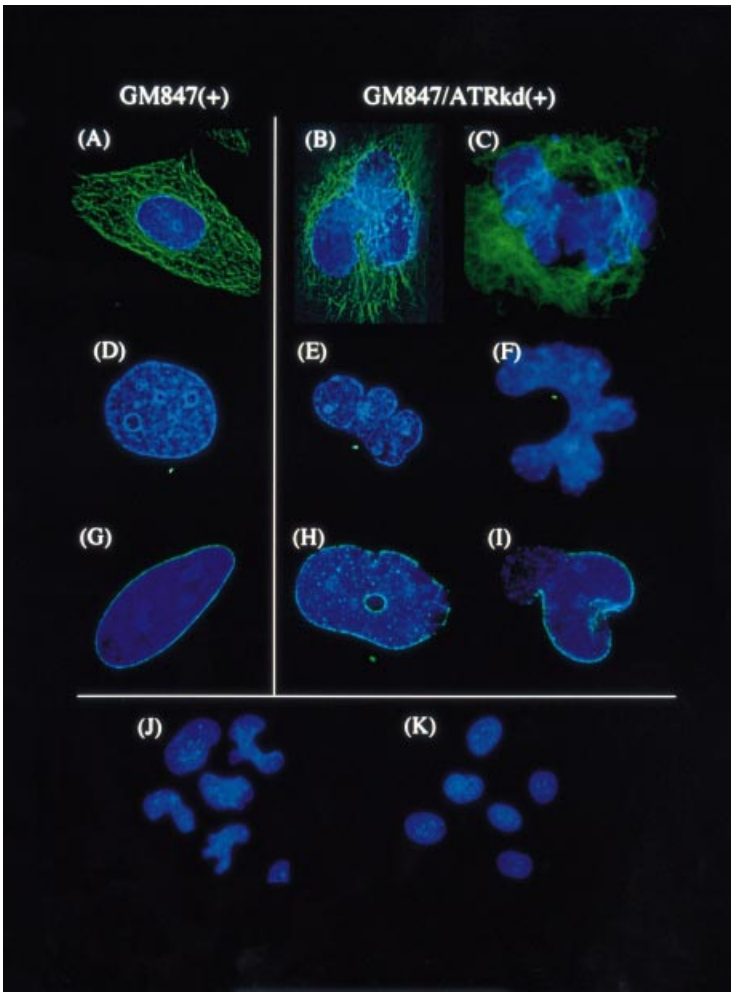

Fig. 6. The effects of hydroxyurea in cells expressing ATRkd. GM847(+) and GM847/ATRkd(+) fibroblasts were treated with 1 mM HU for 24 h and processed for immunofluorescent staining. Cells were stained with anti-α-tubulin (microtubule, **A**–**C**, **J** and **K**), anti-γ-tubulin (centrosomes, **D**–**F**), and anti-lamin B (nuclear lamina, **G**–**I**) antibodies. Bound antibodies were revealed with goat anti-mouse antibodies cross-linked to FITC (green). DNA was counterstained with Hoechst 33258 (blue). Examples of GM847(+) fibroblasts treated with HU are shown in (A), (D) and (G). Examples of GM847/ATRkd(+) fibroblasts treated with HU are shown in (B), (C), (E), (F), (H) and (I). In cells treated with HU either with or without ATRkd, the chromosomes are not condensed (A–I), and a single centrosome is seen (D–F). In a subset of the GM847/ATRkd cells treated with HU, unusual nuclear morphologies are observed. Large invaginations of the nuclei are often observed, giving a bi- and multi-lobed appearance to the nuclei in cells expressing ATRkd (see Table I for quantitation; B, C, E, F, H and I), and are associated with microtubules (B and C). The invaginations line up with the position of the centrosome (E and F), suggesting a role for the microtubular structure in these distortions. The nuclear lamina is focally disrupted in these abnormal nuclei (H and I). Development of the gross abnormalities of the nucleus seen in GM847/ATRkd(+) cells treated with HU (J) are entirely blocked by coincident treatment with the microtubule-depolymerizing drug nocodazole (K). This strongly suggests a causative role for the microtubules in creating the nuclear invaginations and distortions.

ATR and the response to other forms of DNA damage

In addition to moderate IR sensitivity, induction of ATRkd expression renders fibroblasts very sensitive to MMS and *cis*-platinum but only slightly UV sensitive. In contrast, AT fibroblasts are extremely sensitive to IR, but show little or no sensitivity to MMS and UV. Thus, ATM and ATR appear to play complementary roles in the response to different types of DNA damage. The spectrum of DNA damage sensitivities induced by ATR disruption also differs from the *mec1*^{Sc} mutant, which is very sensitive to IR, UV and MMS (Kato and Ogawa, 1994; Weinert *et al.*, 1994). Although it appears that neither ATM nor ATR is required for survival after UV, an alternative explanation may be that ATR and ATM are functionally redundant for responding to UV damage. In this scenario, only a double null cell would show greatly increased UV sensitivity. We did not examine the effect of overexpression of ATRkd on progression through S-phase (S-phase checkpoint) or the G_2 arrest that may accompany other forms of DNA damage. However, given that ATR is required for checkpoint responses to IR and possibly to HU, it is not unreasonable to suppose it is required for the checkpoint responses to the DNA damage produced by these agents.

ATR, HU sensitivity and the DNA replication checkpoint

mec1^{Sc} and *rad3*^{Sp} mutants are HU sensitive and are thought to be defective for the DNA replication checkpoint that coordinates the onset of mitosis and the completion of DNA replication. *mec1*^{Sc} cells show an aberrant spindle elongation in the absence of a fully replicated genome, and *rad3*^{Sp} mutants display an elongated spindle and a cut phenotype (Enoch and Nurse, 1990; Enoch *et al.*, 1992;

Table I. Effect of HU treatment on nuclear morphology

(**A**) Abnormal nuclear morphology after HU treatment

	Untreated	HU
GM847(+)	8.6 ± 2.1	9.9 ± 3.9
GM847/ATRkd(+)	13.6 ± 2.0	30.2 ± 4.3

(**B**) Effect of nocodazole on nuclear morphology after 24 h of HU treatment in GM847/ATRkd(+) cells

	Untreated	Nocodazole	HU	HU + Nocodazole
Mitotic nuclei	7.6 ± 3.1	45.7 ± 17	2.9 ± 3.6	2.7 ± 3.9
Abnormal nuclei	9.0 ± 2.9	5.2 ± 2.8	27.2 ± 4.8	2.7 ± 0.8

Prior to treatment, all cells were grown in the presence of doxycycline for 24 h. For analysis, cells were fixed and analyzed by indirect immunofluorescence as explained in Materials and methods. A minimum of 150 cells were counted by two independent observers for each data point and consistent results were obtained between experiments. (**A**) The percentage of interphase nuclei displaying multiple lobes or deep invaginations after 24 h of treatment with 1 mM HU increases significantly in cells expressing ATRkd. Values are averages of three separate experiments. (**B**) Cells were treated with 1 mM HU, 100 ng/ml nocodazole or both for 24 h and the percentage of nuclei showing condensed chromatin (mitotic) and abnormal nuclear morphologies was determined. Nocodazole prevents the HU-induced increase in abnormal nuclei in cells expressing ATRkd. Comparing treatment with nocodazole alone with treatment with nocodazole and HU reveals that ATRkd-expressing cells are able to arrest prior to chromatin condensation. Values are derived from two independent experiments.

Weinert *et al.*, 1994). We observe that ATRkd expression results in HU sensitivity and a significant increase in irregularly shaped, multi-lobed nuclei in the presence of HU (Figure 6; Table I). The increase in abnormal nuclei of ATRkd cells after HU exposure is not seen when cells are treated with nocodazole, indicating that this is, at least in part, a microtubule-mediated event (Figure 6; Table I). By analogy with yeast, these observations might indicate the onset of mitotic microtubule activities without a replicated genome, condensed chromosomes or nuclear envelope breakdown. To characterize this further, we examined several morphologic characteristics that accompany entry into mitosis. After HU treatment, we did not observe the duplication of centrosomes, condensation of chromatin or the formation of a defined mitotic spindle, but do find partial disruption of nuclear lamina associated with the abnormal nuclei (Figure 6). One model to explain these observations is that expression of ATRkd disrupts the DNA replication checkpoint, resulting in the uncoupling of some but not all mitotic events from the completion of DNA replication. However, HU sensitivity does not necessarily imply a defect in the replication checkpoint. For example, the *rqh1*/*hus2* mutant of *S.pombe* is HU sensitive but not deficient for the DNA replication checkpoint; rather, it has been proposed that *rqh1*+ is required to prevent inappropriate recombination and thus is necessary for recovery from S-phase arrest (Stewart *et al.*, 1997). In addition, several *S.cerevisiae* mutants deficient for double strand break repair are HU sensitive (Allen *et al.*, 1994). It is also possible that ATR is not only required to signal cell cycle arrest, but also plays a direct role in DNA repair, as has been suggested for the Rad3 protein (Jiminez *et al.*, 1992).

PIK-related kinases: regulators of eukaryotic checkpoint functions

We have begun to define the functions of ATR in human cells by engineering cells able to inducibly overexpress wild-type and mutant forms of the protein. To allow selection and maintenance of stable transfectants for these experiments, we used SV40-transformed fibroblast lines from normal and AT individuals. While it has been shown that SV40-transformed AT cells retain the characteristic radiosensitivity and RDS phenotypes relative to control cells (Arlett *et al.*, 1988), it is known that SV40 T-antigen binds to important cell cycle control proteins, including p53 (Nevins, 1994). Our results must be interpreted with this in mind. The strength of this approach is that the tet-inducible ATRkd expression system allows us to alter one variable in these cells and make valid conclusions about ATR function.

ATR is required for the normal response to IR, MMS, *cis*-platinum and HU. In budding and fission yeast, cell cycle arrest in response to a range of DNA-damaging agents requires the two PIK-related kinases $MEC1^{Sc}$ and $Rad3^{Sp}$, respectively. It appears that the homologous pair of proteins in humans, ATM and ATR, are also required for appropriate response to a range of DNA-damaging agents. In at least one case (IR), sensitivity correlates with a lack of arrest, and it is plausible that increases in sensitivity to the other agents may also be due to inabilities to arrest after exposure. Additionally, disruption of ATR function in an AT cell line results in loss of viability, suggesting that the two proteins may share an essential function.

The loss of the ATM gene product results in increased genome instability and an associated increase in cancer. Based on our results, it is likely that loss of ATR would similarly destabilize the genome and may also lead to an increased risk of cancer. It will be of interest to investigate the role of ATR in the onset of cancer. More directly, the inability to stably express ATRkd in AT cells and multiple tumor lines might represent a combination of genetic checkpoint defects not tolerated by human cells. Given that normal fibroblasts appear to tolerate ATR disruption/expression well, this may allow for a distinct therapeutic advantage against cancer cells, because of their inherent genomic instability.

Materials and methods

Construction of tetracycline-inducible ATRwt and ATRkd vectors

The 8.4 kb full-length ATR cDNA was assembled in pBSKII (Stratagene) from pBS-FRP1d, pBS-FRP1c and pBS-FRP1a (Cimprich *et al.*, 1996), such that a *Not*I site was placed immediately upstream of the initiating methionine codon. A kinase-inactivated allele of ATR (ATRkd) was constructed by first introducing a point mutation (D→A) at residue 2475 in pBS-FRP1a. Using the following primers, the mutation was introduced by PCR (5′ ctt gga gcc cgt cat ggt gaa aat 3′, 5′ atg acg ggc tcc aag ccc cag aat 3′, 5′ gct aac cat act agt cat gaa cca ttt cct gga 3′ and 5′ aga gga tca tgt aga aaa 3′), and the resulting 0.7 kb PCR fragment was digested with *Spe*I and *Ppu*MI then ligated into the 6.2 kb fragment of pBS-FRP1a digested with *Nhe*I and *Ppu*MI. This removed the *Nhe*I site in the FRP1kd mutant. The 2.1 kb *Bgl*II–*Bam*HI fragment of pBS-FRP1a-mut was then ligated into a construct prepared from pBS-FRP1c and pBS-FRP1d to give the entire open reading frame of FRP1. The 8.4 kb *Not*I fragments (containing the ATR ORF and 173 bp of 3′ untranslated sequence) of the FRP1wt and FRP1kd cDNAs were subcloned into the *Not*I site of pBJ5F (a derivative of pBJ5; Clipstone and

Crabtree, 1992), resulting in an in-frame fusion of the FRP open reading frame with 12 amino-terminal residues including an initiating methionine, eight residues comprising the FLAG epitope (Prickett *et al.*, 1989) and three linker amino acids: M-DYKDDDDK-GGR-MG... . The two ATR cDNAs were placed under the control of the tetracycline-inducible tet-promoter by subcloning an 8.5 kb *Bam*HI fragments (containing 135 bp of 5′ untranslated sequence, the ATRwt or ATRkd coding sequence and 161 nucleotides of 3′ untranslated sequence) from pBJF-FRPwt or pBJF-FRPkd into the *Bam*HI sites of pUHD10-3 (Gossen and Bujard, 1992), creating ptetATRwt and ptetATRkd, respectively.

Cell lines and transfections

GM847 is an SV40-transformed fibroblast line from a normal individual and is a kind gift from Ray Monnat (Department of Pathology, University of Washington, Seattle, WA). AT3BI and AT4BI are SV40-transformed fibroblasts from homozygous ataxia telangiectasia patients and were obtained from Patrick Concannon (Virginia Mason Research Center, Seattle, WA). All stable clones were derived after transfection of the parental GM847 line. All cells were maintained in Dulbecco's modified Eagle's medium (DMEM) with 4.5 g/l glucose, supplemented with 10% fetal calf serum (Hyclone) and L-glutamine. Cells were grown at 37°C in 5% CO_2.

A calcium phosphate transfection kit (Gibco BRL) was used according to the manufacturer's recommendation. 2 μg of *Pvu*II-linearized pUHD172.1neo (generously provided by Dr Pearl Huang), encoding the reverse tet-transcriptional activator and neomycin resistance (rtTA; Gossen *et al.*, 1995), were co-transfected with 10 μg of either *Pvu*I-linearized ptetATRwt or ptetATRkd into 10 cm plates containing 2×10^6 cells. After 4 h, cells were exposed for 3 min to 15% glycerol, washed three times in phosphate-buffered saline (PBS) and fed with non-selective medium. At 24 h after transfection, cells were split 1:6 into selection medium containing 400 μg/ml of G418 (Gibco BRL), and stable clones were picked at 3–5 weeks. To induce transcription from the tet-responsive constructs, doxycycline (Sigma) was added to the medium at 1 μg/ml. Clones were screened by immunoblotting for the ability to express the FLAG-ATR construct in the presence of doxycycline but show minimal expression in its absence. All clones were maintained in selection medium without doxycycline. Prior to all experiments, cells were split into media with or without doxycycline for 24 h and expression of protein analyzed by Western blotting.

Western analysis and kinase assay

Cells were grown to 80% confluence and split into media ± doxycycline. After 24 h, cells were harvested, total cellular extracts were prepared and total protein was resolved by SDS–PAGE. Anti-FLAG M5 antibody (Eastman Kodak Company), which specifically recognizes the N-terminal FLAG epitope adjacent to the first methionine codon, was used according to the manufacturer's instructions. Detection was performed by the enhanced chemiluminescence system (Amersham). To determine the increase in ATR expression levels achieved upon induction, equal amounts of total protein from ATR(–) and ATR(+) samples were resolved by SDS–PAGE and probed with anti-ATR antibody. Autoradiographs were scanned using a GS-700 Imaging Densitometer (Bio-Rad), and the ratio of band intensity analyzed by Molecular Analyst software (Bio-Rad).

For kinase assays, three plates (15 cm) of each cell line were grown in media containing 1 mg/ml doxycycline for 24 h. Cells were trypsinized and washed three times in cold PBS and the pellet was lysed for 15 min at 4°C in 450 μl of lysis buffer [MIPP buffer (2 mM EDTA, 2 mM EGTA, 25 mM NaF, 100 mM Na_3VO_4, 25 mM 2-glycerophosphate, 1 μg/ml leupeptin, 1 μg/ml pepstatin), 450 mM NaCl, 1% Triton X-100, 1 mM dithiothreitol (DTT), 0.4 mM pefablock]. Clarified lysates were diluted with 700 μl of MIPP, 0.5% Triton X-100, 1 mM DTT. Expressed proteins were immunoprecipitated (1.5 h at 4°C) with anti-FLAG M2 antibody affinity gel (Eastman Kodak Company), and the complexes were washed three times with lysis buffer, once with MIPP, 0.5% Triton-X, 500 mM LiCl, 1 mM DTT and once with kinase reaction buffer (25 mM HEPES pH 7.4, 50 mM NaCl, 20% glycerol, 0.1% NP-40, 10 mM $MgCl_2$, 1 mM DTT). The beads were then resuspended in 20 μl of kinase buffer containing 100 μM cold ATP and 10 μCi of γ-labeled [^{32}P]ATP. The mixture was incubated at 30°C for 12 min with vigorous shaking. Then 30 μl of 2× SDS sample buffer were added, and the phosphorylated proteins were separated by SDS–PAGE and transferred to PVDF membranes for autoradiography and detection with anti-FLAG M2 antibody.

Irradiation and chemicals

Irradiation was performed at room temperature using a ^{137}Cs source delivering γ-rays at a dose rate of 3.4 Gy/min. UV exposure was performed at room temperature at a dose rate of 1.5 J/m^2. Unless otherwise noted, chemicals were obtained from Sigma Chemical Company. MMS and anti-Flag antibody were obtained from Kodak. 4′,6′-Diamidino-2-phenylindole (DAPI) and anti-mouse antibody were obtained from Boehringer Mannheim. RNase cocktail was obtained from Ambion Inc. Doxycycline was obtained from Gibco BRL. The polyclonal anti-ATR antibody was raised against a peptide at the N-terminus of ATR.

Clonogenic survival assays

Cells were plated in triplicate in 6 cm Petri dishes into complete medium ± doxycycline (0.1 μg/ml) at 37°C, 5% CO_2. Following a 24 h incubation, cells were treated with irradiation or chemical agents then incubated for 10–14 days. After colony formation, cells were fixed with 3.7% formaldehyde and stained with 0.1% crystal violet. Colony formation was determined by counting the number of colonies with >50 cells per plate. Clonogenic survival data show results from at least two independent experiments. For each independent experiment, averages and standard deviations were determined from triplicates. Plating efficiencies were determined for each cell line with and without doxycycline. Treated sample percentages were determined by dividing their plating efficiency by the plating efficiency of the appropriate untreated control.

G_2/M checkpoint assay

Cells were plated at 1×10^5/ml in complete media ± doxycycline (0.1 μg/ml) at 37°C, 5% CO_2. Following overnight incubation, cells were treated with 8 Gy γ-radiation ± nocodazole (0.1 μg/ml), then placed at 37°C, 5% CO_2 for 16 h. After incubation, cells were harvested (floating and attached), pelleted at 800 *g* and resuspended in 2 ml of PBS. Each sample was then divided into two separate sets, either for mitotic index or DNA content determination, and repelleted at 800 *g*. For DNA content determination, samples were resuspended in 1 ml of hypotonic staining solution (0.1% sodium citrate, 0.1% Triton X-100, 50 μg/ml propidium iodide and 1 mg/ml RNase cocktail) at 4°C overnight. Following staining, cell cycle analysis of DNA content was performed using a Becton Dickinson FACSCAN equipped with Cellquest software (Becton Dickinson). Ten thousand cells were analyzed for each point. Cell cycle distribution and percentages were determined using the Multicycle AV cell cycle program (Phoenix Flow Systems, Inc. ©1994; graciously provided by Peter Rabinovitch, Department of Pathology, University of Washington, Seattle, WA). Standard deviations for cell cycle percentages based on DNA content were determined from four separate experiments. For mitotic index determination, mitotic spreads were prepared as described previously (Anderson and Roberge, 1992). Briefly, samples were resuspended in 1 ml of 75 mM KCl for 10 min, pelleted, resuspended in Carnoy's fixative (1:3 v/v acetic acid:methanol) and incubated for 10 min at room temperature or 2 days at 4°C. Following fixation, all but ~20 μl of supernatant was discarded, and the pellets were resuspended in the remaining volume, spotted onto glass slides and allowed to air dry. Once dry, samples were stained with 1 μg/ml DAPI for 5 min, drained and allowed to air dry again before addition of 5 μl of anti-fade (90% glycerol and 0.2 M *n*-propylgallate in PBS). Coverslips were then placed over anti-fade and sealed. Mitotic cell analysis was performed using a fluorescent microscope. Four hundred cells were counted on each sample. Standard deviations for mitotic index percentages were determined from four separate experiments. Finally, the G_2 cell cycle percentage was determined by subtracting the percentage mitotic cells from the G_2/M cell cycle percentage attained from Multicycle AV.

DNA synthesis assays

Cells were plated at 1×10^5/ml in complete medium with 0.02 μCi/ml of [^{14}C]thymidine ± doxycycline (0.1 μg/ml). Following 48 h incubation at 37°C in 5% CO_2, cells were treated with γ-radiation at 0.5–40 Gy or HU at 0.25–10 mM. After treatment, cells were washed twice with PBS and placed in complete medium with 2.5 μCi/ml of [^{3}H]thymidine. Cells were then incubated for an additional 4 h. Following incubation, samples were washed twice with PBS and lysed with 0.3 ml of 2% SDS. Each sample was then drawn through a 0.22 gauge syringe twice and spotted onto Whatman filter paper strips. Each filter strip was then washed sequentially with 5% trichloroacetic acid (TCA), 90% EtOH and 95% EtOH for 5 min at each step and allowed to air dry overnight. Once dry, filter strips were placed into scintillation vials with 5 ml of Microscint-2. Scintillation vials were then read on the scintillation counter for ^{3}H and ^{14}C c.p.m. with standards for each isotope. The c.p.m. values were

corrected for crossover based on standards. Averages and standard deviations were determined from triplicate samples. Final results were presented in percentage DNA synthesis by first determining the ratio of ^{3}H to ^{14}C and then normalizing the treated samples to the appropriate untreated control.

Immunofluorescence

Cells were plated onto glass coverslips pre-treated with poly-L-lysine at 1×10^{4} cells/cm^{2}. After 24 h, either 1 mM HU or 20 μM aphidicolin was added and coverslips were processed at designated time points. Cells were extracted for 30 s in pre-warmed buffer containing 80 mM PIPES pH 6.8, 1 mM $MgCl_2$, 4 mM EGTA. For immunodetection of microtubule structures, cells were fixed in 0.5% glutaraldehyde for 10 min. Cells were treated with 0.1% $NaBH_4$ in PBS for 7 min to quench the unreacted glutaraldehyde, and rinsed well in PBS. Immunodetection was then carried out using anti-tubulin antibody at a 1:200 dilution, (DM1alpha, Sigma) and fluorescein-labeled secondary antibody (1:200 dilution). DNA was stained with 1 μg/ml Hoechst 33258 stain and coverslips were mounted on glass slides. For visualization of centrioles and nuclear lamin, the protocol was modified as follows: cells were fixed in ice-cold methanol for 3 min, rinsed well in PBS and processed for γ-tubulin or lamin B immunofluorescence using anti-γ-tubulin antibody (GTU-88, Sigma) or anti-lamin B antibody (CalBiochem) respectively. A minimum of 150 total cells were counted by two independent observers to derive percentages of abnormal nuclei. All experiments were performed at least twice.

Acknowledgements

We are especially indebted to Sondra Goehle for expert technical support. We also thank Peter Rabinovich for advice and assistance with flow cytometry; Andrew Murray for insightful discussions; Ted Weinert, Amanda Paulovich, Jim Roberts, John Petrini and Leland Hartwell for comments on the manuscript; and members of the Seattle Project for advice and suggestions during this work. This work was supported by Merck and Co. W.A.C. received support from Karl Podratz and a research fellowship from Mayo Foundation. K.A.C. was supported by a post-doctoral fellowship from the Damon Runyon-Walter Winchell Foundation for Cancer Research.

References

Allen,J.B., Zhou,Z., Siede,W., Friedberg,E.C. and Elledge,S.J. (1994) The SAD1/RAD53 protein kinase controls multiple checkpoints and DNA damage-induced transcription in yeast. *Genes Dev.*, **8**, 2401–2415.

Anderson,H.J. and Roberge,M. (1992) DNA topoisomerase II: a review of its involvement in chromosome structure, DNA replication, transcription and mitosis. *Cell Biol. Int. Rep.*, **16**, 717–724.

Arlett,C.F., Green,M.H., Priestley,A., Harcourt,S.A. and Mayne,L.V. (1988) Comparative human cellular radiosensitivity: I. The effect of SV40 transformation and immortalisation on the gamma-irradiation survival of skin derived fibroblasts from normal individuals and from ataxia-telangiectasia patients and heterozygotes. *Int. J. Radiat. Biol.*, **54**, 911–928.

Bentley,N.J., Holtzman,D.A., Flaggs,G., Keegan,K.S., DeMaggio,A., Ford,J.C., Hoekstra,M.F. and Carr,A.M. (1996) The *Schizosaccharomyces pombe rad3* checkpoint gene. *EMBO J.*, **15**, 6641–6651.

Brown,E.J. and Schreiber,S.L. (1996) A signaling pathway to translational control. *Cell*, **86**, 517–520.

Brown,E.J., Beal,P.A., Keith,C.T., Chen,J., Shin,T.B. and Schreiber,S.L. (1995) Control of p70 S6 kinase by kinase activity of FRAP *in vivo*. *Nature*, **377**, 441–446.

Carr,A.M. (1997) Control of cell cycle arrest by the $Mec1^{Sc}$/$Rad3^{Sp}$ DNA structure checkpoint pathway. *Curr. Opin. Genet. Dev.*, **7**, 93–98.

Cimprich,K.A., Shin,T.B., Keith,C.T. and Schreiber,S.L. (1996) cDNA cloning and gene mapping of a candidate human cell cycle checkpoint protein. *Proc. Natl Acad. Sci. USA*, **93**, 2850–2855.

Clipstone,N.A. and Crabtree,G.R. (1992) Identification of calcineurin as a key signalling enzyme in T-lymphocyte activation. *Nature*, **357**, 695–697.

Dasso,M. and Newport,J.W. (1990) Completion of DNA replication is monitored by a feedback system that controls the initiation of mitosis *in vitro*: studies in *Xenopus*. *Cell*, **61**, 811–823.

Elledge,S.J. (1996) Cell cycle checkpoints: preventing an identity crisis. *Science*, **274**, 1664–1672.

Enoch,T. and Nurse,P. (1990) Mutation of fission yeast cell cycle control genes abolishes dependence of mitosis on DNA replication. *Cell*, **60**, 665–673.

Enoch,T., Carr,A.M. and Nurse,P. (1992) Fission yeast genes involved in coupling mitosis to completion of DNA replication. *Genes Dev.*, **6**, 2035–2046.

Gossen,M. and Bujard,H. (1992) Tight control of gene expression in mammalian cells by tetracycline-responsive promoters. *Proc. Natl Acad. Sci. USA*, **89**, 5547–5551.

Gossen,M., Freundlieb,S., Bender,G., Muller,G., Hillen,W. and Bujard,H. (1995) Transcriptional activation by tetracyclines in mammalian cells. *Science*, **268**, 1766–1769.

Greenwell,P.W., Kronmal,S.L., Porter,S.E., Gassenhuber,J., Obermaier,B. and Petes,T.D. (1995) *TEL1*, a gene involved in controlling telomere length in *S.cerevisiae*, is homologous to the human Ataxia telangiectasia gene. *Cell*, **82**, 823–829.

Hall,M.N. (1996) The TOR signalling pathway and growth control in yeast. *Biochem. Soc. Trans.*, **24**, 234–239.

Hari,K.L., Santerre,A., Sekelsky,J.J., McKim,K.S., Boyd,J.B. and Hawley,R.S. (1995) The *mei-41* gene of *D.melanogaster* is a structural and functional homolog of the human Ataxia telangiectasia gene. *Cell*, **82**, 815–821.

Hartwell,L.H. and Kastan,M.B. (1994) Cell cycle control and cancer. *Science*, **266**, 1821–1828.

Hawley,R.S. and Friend,S.H. (1996) Strange bedfellows in even stranger places: the role of ATM in meiotic cells, lymphocytes, tumors, and its functional links to p53. *Genes Dev.*, **10**, 2383–2388.

Hoekstra,M.F. (1997) Responses to DNA damage and regulation of cell cycle checkpoints by the ATM protein kinase family. *Curr. Opin. Genet. Dev.*, **7**, 170–175.

Jackson,S.P. (1996a) DNA damage detection by DNA dependent protein kinase and related enzymes. *Cancer Surv.*, **28**, 261–279.

Jackson,S.P. (1996b) The recognition of DNA damage. *Curr. Opin. Genet. Dev.*, **6**, 19–25.

Jimenez,G., Yucel,J., Rowley,R. and Subramani,S. (1992) The *rad3+* gene of *Schizosaccharomyces pombe* is involved in multiple checkpoint functions and in DNA repair. *Proc. Natl Acad. Sci. USA*, **89**, 4952–4956.

Kastan,M.B. (1996) Signalling to p53: where does it all start?. *BioEssays*, **18**, 617–619.

Kastan,M.B., Zhan,Q., el-Deiry,W.S., Carrier,F., Jacks,T., Walsh,W.V., Plunkett,B.S., Vogelstein,B. and Fornace,A.J. (1992) A mammalian cell cycle checkpoint pathway utilizing p53 and GADD45 is defective in ataxia-telangiectasia. *Cell*, **71**, 587–597.

Kato,R. and Ogawa,H. (1994) An essential gene, *ESR1*, is required for mitotic cell growth, DNA repair and meiotic recombination in *Saccharomyces cerevisiae*. *Nucleic Acids Res.*, **22**, 3104–3112.

Keegan,K.S. *et al*. (1996) The Atr and Atm protein kinases associate with different sites along meiotically pairing chromosomes. *Genes Dev.*, **10**, 2423–2437.

Keith,C.T. and Schreiber,S.L. (1995) PIK-related kinases: DNA repair, recombination, and cell cycle checkpoints. *Science*, **270**, 50–51.

Kinzler,K.W. and Vogelstein,B. (1996) Lessons from hereditary colorectal cancer. *Cell*, **87**, 159–70.

Kumagai,A. and Dunphy,W.G. (1995) Control of the Cdc2/cyclin B complex in *Xenopus* egg extracts arrested at a G_2/M checkpoint with DNA synthesis inhibitors. *Mol. Biol. Cell*, **6**, 199–213.

Levine,A.J. (1997) p53, the cellular gatekeeper for growth and division. *Cell*, **88**, 323–331.

Lew,D.J. and Kornbluth,S. (1996) Regulatory roles of cyclin dependent kinase phosphorylation in cell cycle control. *Curr. Opin. Cell Biol.*, **8**, 795–804.

Linke,S.P., Clarkin,K.C., KiLeonardo,A., Tsou,A. and Wahl,G.M. (1996) A reversible, p53-dependent G_0/G_1 cell cycle arrest induced by ribonucleotide depletion in the absence of detectable DNA damage. *Genes Dev.*, **10**, 934–947.

Lydall,D. and Weinert,T. (1996) From DNA damage to cell cycle arrest and suicide: a budding yeast perspective. *Curr. Opin. Genet. Dev.*, **6**, 4–11.

Meyn,M.S. (1995) Ataxia-telangiectasia and cellular responses to DNA damage. *Cancer Res.*, **55**, 5991–6001.

Morrow,D.M., Tagle,D.A., Shiloh,Y., Collins,F.S. and Hieter,P. (1995) TEL1, an *S.cerevisiae* homolog of the human gene mutated in Ataxia telangiectasia, is functionally related to the yeast checkpoint gene *MEC1*. *Cell*, **82**, 831–840.

Nevins,J.R. (1994) Cell cycle targets of the DNA tumor viruses. *Curr. Opin. Genet. Dev.*, **4**, 130–134.

Painter,R.B. and Young,B.R. (1980) Radiosensitivity in ataxia-telangiectasia: a new explanation. *Proc. Natl Acad. Sci. USA*, **77**, 7315–7317.

Paules,R.S. *et al*. (1995) Defective G_2 checkpoint function in cells from individuals with familial cancer syndromes. *Cancer Res.*, **55**, 1763–1773.

Paulovich,A.G. and Hartwell,L.H. (1995) A checkpoint regulates the rate of progression through S-phase in *S.cerevisiae* in response to DNA damage. *Cell*, **82**, 841–847.

Paulovich,A.G., Toczyski,D.P. and Hartwell,L.H. (1997) When checkpoints fail. *Cell*, **88**, 315–321.

Perlmutter,R.M. and Alberola,I.J. (1996) The use of dominant-negative mutations to elucidate signal transduction pathways in lymphocytes. *Curr. Opin. Immunol.*, **8**, 285–290.

Prickett,K.S., Amberg,D.C. and Hopp,T.P. (1989) A calcium-dependent antibody for identification and purification of recombinant proteins. *Biotechniques*, **7**, 580–589.

Rudner,A.D. and Murray,A.W. (1996) The spindle assembly checkpoint. *Curr. Opin. Cell Biol.*, **8**, 773–780.

Sanchez,Y., Desany,B.A., Jones,W.J., Liu,Q., Wang,B. and Elledge,S.J. (1996) Regulation of *RAD53* by the ATM-like kinases *MEC1* and *TEL1* in yeast cell cycle checkpoint pathways. *Science*, **271**, 357–360.

Savitsky,K., Sfez,S., Tagle,D.A., Ziv,Y., Sartiel,A., Collins,F.S., Shiloh,Y. and Rotman,G. (1995) The complete sequence of the coding region of the ATM gene reveals similarity to cell cycle regulators in different species. *Hum. Mol. Genet.*, **4**, 2025–2032.

Schmidt,A., Kunz,J. and Hall,M.N. (1996) TOR2 is required for organization of the actin cytoskeleton in yeast. *Proc. Natl Acad. Sci. USA*, **93**, 13780–13785.

Seaton,B.L., Yucel,J., Sunnerhagen,P. and Subramani,S. (1992) Isolation and characterization of the *Schizosaccharomyces pombe rad3* gene, involved in the DNA damage and DNA synthesis checkpoints. *Gene*, **119**, 83–89.

Siede,W., Allen,J.B., Elledge,S.J. and Friedberg,E.C. (1996) The *Saccharomyces cerevisiae MEC1* gene, which encodes a homolog of the human ATM gene product, is required for G_1 arrest following radiation treatment. *J. Bacteriol.*, **178**, 5841–5843.

Stewart,E. and Enoch,T. (1996) S-phase and DNA-damage checkpoints: a tale of two yeasts. *Curr. Opin. Cell Biol.*, **8**, 781–787.

Stewart,E., Chapman,C.R., Al,K.F., Carr,A.M. and Enoch,T. (1997) *rqh1+*, a fission yeast gene related to the Bloom's and Werner's syndrome genes, is required for reversible S-phase arrest. *EMBO J.*, **16**, 2682–2692.

Weaver,D.T. (1995) What to do at an end: DNA double-strand-break repair. *Trends Genet.*, **11**, 388–392.

Weinert,T.A., Kiser,G.L. and Hartwell,L.H. (1994) Mitotic checkpoint genes in budding yeast and the dependence of mitosis on DNA replication and repair. *Genes Dev.*, **8**, 652–665.

Zheng,X.F., Florentino,D., Chen,J., Crabtree,G.R. and Schreiber,S.L. (1995) TOR kinase domains are required for two distinct functions, only one of which is inhibited by rapamycin. *Cell*, **82**, 121–130.

Received August 11, 1997; revised October 8, 1997; accepted October 14, 1997